International Journal for Multidisciplinary Research (IJFMR)
E-ISSN: 2582-2160 ● Website: www.ijfmr.com ● Email: editor@ijfmr.com

Glycol Mediated Synthesis of Green Rust, Its Delamination and Solvothermal Decomposition of the Resulting Colloidal Dispersion to Form Monodispersed Γ-Fe_2O_3 Nanoparticles

Jyothi Sequeira

Assistant Professor, Applied Science Department, Usha Mittal institute of Technology, SNDT Women's University

Abstract

Hydroxychloride green rust was synthesized by urea hydrolysis of ferric chloride in ethylene glycol. The chloride ions of green rust were then exchanged with the surfactant anion, dodecylsulphate (DS). Surfactant-intercalated green rust (GRDS) delaminated in 1,2-propanediol to give a stable colloidal dispersion of monolayers. Solvothermal decomposition of the colloidal dispersion resulted in monodispersed, single crystalline meghamite, γ-Fe_2O_3 nanoparticles of ~10 nm diameter.

Keywords: Hydroxychloride green rust, delamination, γ-Fe_2O_3 nanoparticles

Graphical abstract

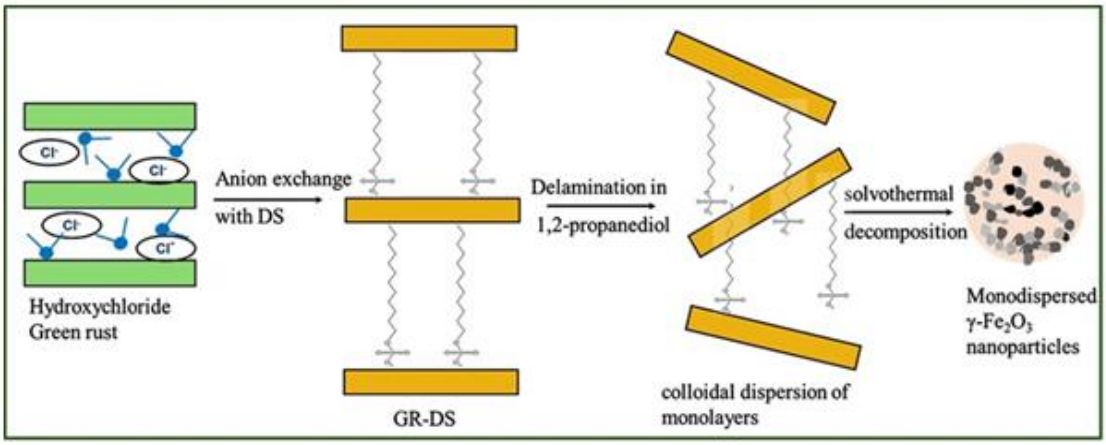

1. Introduction

Green crystalline chemical compounds, having a layered double hydroxide (LDH) structure consisting of iron(II) and iron(III) hydroxide layers and the interlayers occupied with loosely held anions and water molecules are known as Geen rusts (GR) [1]. Their composition confers interesting redox properties making them important in the areas such as corrosion of iron-based materials, environmental science and mineralogy. These have positively charged brucite-like layers of the composition $[Fe\ (II)_{(1-x)}\ Fe\ (III)_x(OH)_2]^{2+}$ that alternate with interlayers made of anions (such as CO_3^{2-}, SO_4^{2-}, Cl^-) and water molecules

[2, 3]. GR can either occur naturally in slightly reducing environments such as hydromorphic soils [4]; formed as the intermediate product of aqueous [5, 6, 7], atmospheric [8] or marine [9] corrosion of iron or steel or they can also be prepared in the laboratory [1, 3, 10, 11]. Though anion exchange reactions in LDHs have been well studied [12], among GR these reactions have not been explored well [13] as these systems are quite sensitive to oxidation and hence difficult to handle. Delamination of GR has also not been reported, possibly for the same reason. It is of interest therefore to carry out suitable anion exchange reactions in GR which would facilitate the delamination of these LDHs.

Delamination is a phenomenon studied thoroughly among the layered solids where the individual layers of a layered solid come apart to give a stable colloidal dispersion of monolayers in a suitable solvent [14]. Depending on the layer charge density, layered solids can be delaminated either in water or in organic solvents. LDHs contain positively charged layers and negatively charged intercalating anions. They have high charge density and strong interlayer hydrogen bonding, hence do not easily delaminate in solvents [15]. Studies have shown that on modifying the interlayer of the LDHs with hydrophobic/hydrophilic guest species as anions, they delaminate in organic solvents or water [16, 17, 18]. Colloidal dispersion obtained by the delamination of layered hydroxides in suitable solvents has become a potential method to prepare new materials such as composites and nanomaterials [19, 20, 21]. The same principle is employed in this work to obtain iron oxide nanoparticles from the colloidal dispersion containing monolayers of surfactant intercalated green rust through solvothermal decomposition.

Superparamagnetic iron oxide nanoparticles (generally abbreviated as SPIONS) of γ-Fe_2O_3 (maghemite) or Fe_3O_4 (magnetite) are suitable candidates for applications such as ferrofluids, color imaging, magnetic refrigeration, detoxification of biological fluids, magnetically controlled transport of anticancer drugs, MRI contrast enhancement and magnetic cell separation, biosensors, high density magnetic storage devices and catalysis [22, 23]. γ-Fe_2O_3 is found in nature as the mineral maghemite. Maghemite is an inverse spinel with a cubic unit cell (a=8.351 A, space group $P4_132$) containing cations in tetrahedral A and octahedral B positions, to compensate for the increased positive charge there are vacancies usually in the octahedral positions. Stoichiometric Fe_2O_3 has a formula $Fe^A(Fe_{5/3}[]_{1/3})^BO_4$. Synthetic maghemite has a superstructure originating from cation and vacancy ordering which causes a reduction in the symmetry from cubic to tetragonal. (a= 8.33, c= 25.01). Bulk maghemite is a typical representative of ferromagnetic materials. Nanocrystalline γ-Fe_2O_3 is one of the first materials to show superparamagnetic relaxation [22].

This study presents a new synthetic route to hydroxychloride green rust (GRCl) through the hydrolysis of iron chloride in a polyol medium. The obtained GRCl was then subjected to anion exchange reaction using a surfactant, dodecyl sulfate (DS) anion in ethanol. The DS intercalated GR (GRDS) could be delaminated in organic solvents such as 1,2- propanediol and the dispersion of GRDS thus obtained containing solvated monolayers could be subjected to solvothermal decomposition to get monodispersed superparamagnetic γ- Fe_2O_3 nanoparticles.

2. Experimental section

2.1 Preparation of hydroxychloride green rust (GRCl)

A mixture of 1 g of $FeCl_3.6H_2O$ (0.0037 mol), 0.222 g of urea (0.0037 mol) and 1.4 cm^3 n-octylamine was added to 50 cm^3 of ethylene glycol in a 250 cm^3 round bottomed flask and the mixture refluxed for 1 h. The green solid obtained was separated by centrifugation and washed with 1-propanol five times followed by diethyl ether two times. The solid was dried at room temperature and stored under vacuum.

2.2 Anion exchange reaction of GRCl

The as prepared GRCl, Fe (II)$_3$Fe (III)(OH)$_8$Cl.2H$_2$O, was subjected to anion exchange reaction with surfactant anion, dodecylsulfate (DS). About 2 g of GRCl was added to a solution containing 9.64 g of sodium dodecylsulphate in 50 cm^3 of ethanol and the mixture was stirred at room temperature for 5 days. Initially the mixture was green in color but turned yellow within 24 h. The resultant solid, dodecylsulfate intercalated green rust (GRDS), was separated by centrifugation, washed with 1-propanol several times and dried in air at room temperature to constant mass.

2.3 Delamination of GRDS

About 50 mg of the surfactant intercalated GRDS was dispersed in 100 cm^3 of various solvents, such as 1-butanol, ethylene glycol and 1,2-propanediol and the resultant mixture in each case was sonicated for 1 h at room temperature. The undispersed solid from the colloidal dispersions thus obtained was removed by centrifuging the dispersion at 2500 rpm. The dispersions were then set aside and their stabilities monitored over a period of 1 month.

The layers from the colloidal dispersions were restacked by adding equal volume of acetone to the dispersion. Complete settling of the solid was observed within 3 h. Solids thus obtained were washed with acetone and dried in air at room temperature to get constant mass.

2.4 Solvothermal decomposition of GRDS dispersion in 1,2-propandiol

About 500 mg of GRDS was dispersed in 50 cm^3 of 1,2-propanediol along with 100 mg of urea and 1 cm^3 of water and the mixture was sonicated for about 30 min. The resultant colloidal dispersion was transferred to a stainless-steel autoclave and heated in a hot air-oven at 200 °C for 24 h. After the reaction the autoclave was cooled to room temperature and the solid product was separated by centrifugation, washed with ethanol followed by acetone and dried at 65 °C to constant mass.

3. Characterization

All the samples were characterized by powder X-Ray diffraction (PANalytical X-pert Pro fitted with a secondary graphite monochromator, CuKα radiation, 2° 2θ/min) and infrared spectroscopy (Nicolet IR200 FTIR spectrometer, KBr pellet, 4 cm^{-1} resolution). Transmission electron microscopy (TEM) images were recorded with a JEOL F3000 microscope operated at 300 kV.

4. Results and discussion

The PXRD pattern of GRCl shown in Figure 1a (and the inset in 1a) matches well with what has been reported for chloride intercalated GR [11, 24]. The basal spacing calculated from the *100* reflections is 0.81 nm. The increased basal spacing of the DS-exchanged green rust, GRDS (Figure 1b) from 0.81 nm to 3.63 nm confirms the intercalation of the large DS ions. The presence of multiple *h00* reflections indicates that the structure is well ordered along the stacking direction. There are a few weak peaks which do not belong to the GR phase in the region 2θ = 20-22° in both the patterns and these could be due to impurities.

In the IR spectrum of GRDS (Figure 2a), there is a band around 3420 cm^{-1} due to the O—H stretching vibrations. There are four skeletal vibrations in the region 400–900 cm^{-1} which are commonly observed in green rust LDHs [25]. The characteristic absorption bands due to C—H stretching at 2950–2850 cm^{-1} and S=O stretching at 1220 cm^{-1} are due to the intercalated DS ion. The observed C—H stretching vibrations suggest that the alkyl chains take up an all-trans conformation [26, 27].

Figure 1: PXRD patterns of the as prepared hydroxychloride green rust, GRCl (a) GRDS obtained by anion exchange (b) and a restacked sample obtained by the addition of acetone to the colloidal dispersion of GRDS in 1,2-propanediol (c). The region 2θ = 25-70 ° is expanded in the inset in (a). The *in situ* XRD of colloidal dispersion of DS-intercalated green rust in 1,2-propanediol is shown as inset in (b).

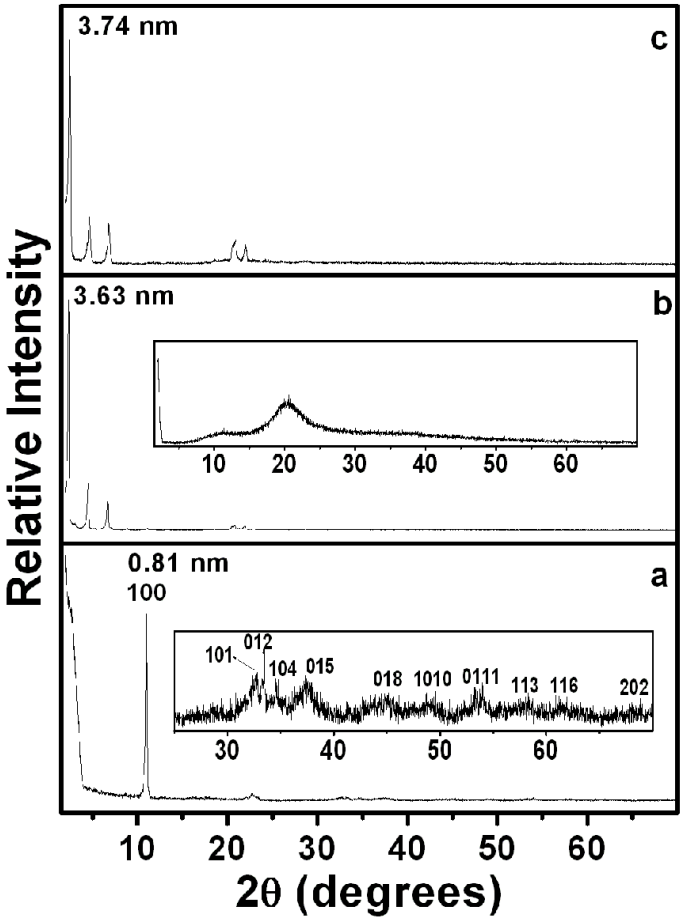

DS intercalated LDHs are known to delaminate readily in alcohols such as 1-butanol [28, 29]. While the hydroxyl ends of the alcohols bind to the inorganic layers through H-bonding their alkyl chains solvate the interlayer organic matter causing effective solvation of the layers leading to exfoliation [28, 29]. Like other DS intercalated LDHs, GRDS too dispersed to give stable translucent solutions upon sonication in solvents such as 1-butanol and 1,2-propanediol. While about 2 g of the LDH could be dispersed in 1 L of 1-butanol about 2.5 g of it got dispersed in 1 L of 1,2-propanediol. Both the dispersions were quite stable. When the dispersions were set aside it took more than a month for half the dispersed material to coagulate. However, when acetone was added to the dispersions the coagulation was rapid and the entire solid settled down within 3 h.

Figure 2: IR spectra of the as prepared GRDS (a) and a restacked sample of GRDS obtained by the addition of acetone to the colloidal dispersion of GRDS (b).

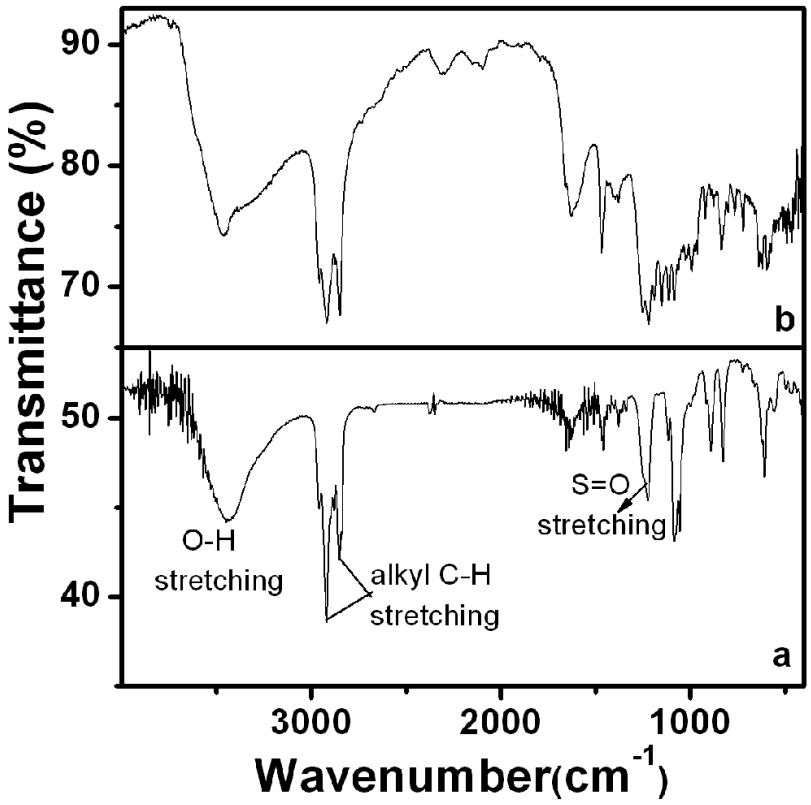

The inset in Figure 1b is the *in situ* PXRD pattern of the colloidal dispersion obtained by dispersing GRDS in 1,2-propanediol. No *h00* reflections are observed here suggesting that the layers have come apart and the dispersion consists of monolayers. The broad peak around $2\theta = 20°$ is due to the sample holder. Figure 1c shows the PXRD pattern of the sample obtained on restacking the layers from the colloidal dispersion of GRDS by adding acetone. The pattern is identical to that of the parent GRDS with a slight increase in the basal spacing from 3.63 to 3.74 nm which could be due to the incomplete removal of the solvent molecules during restacking or due to the modified organization of the surfactant ions in the interlayer gallery. In addition, the peaks are slightly broadened when compared to the parent GRDS suggesting disorder along the stacking direction to a small extent in the restacked sample. The IR spectrum of the restacked GRDS (Figure 2b) shows features similar to that of the parent DS intercalated green rust (Figure 2a) further confirming that the structure of the restacked sample is same as that of the parent GRDS.

Figure 3: The PXRD pattern (a) and IR spectrum (b) of γ-Fe_2O_3 obtained on solvothermal decompostion of GRDS in 1,2-propanediol at 200 °C

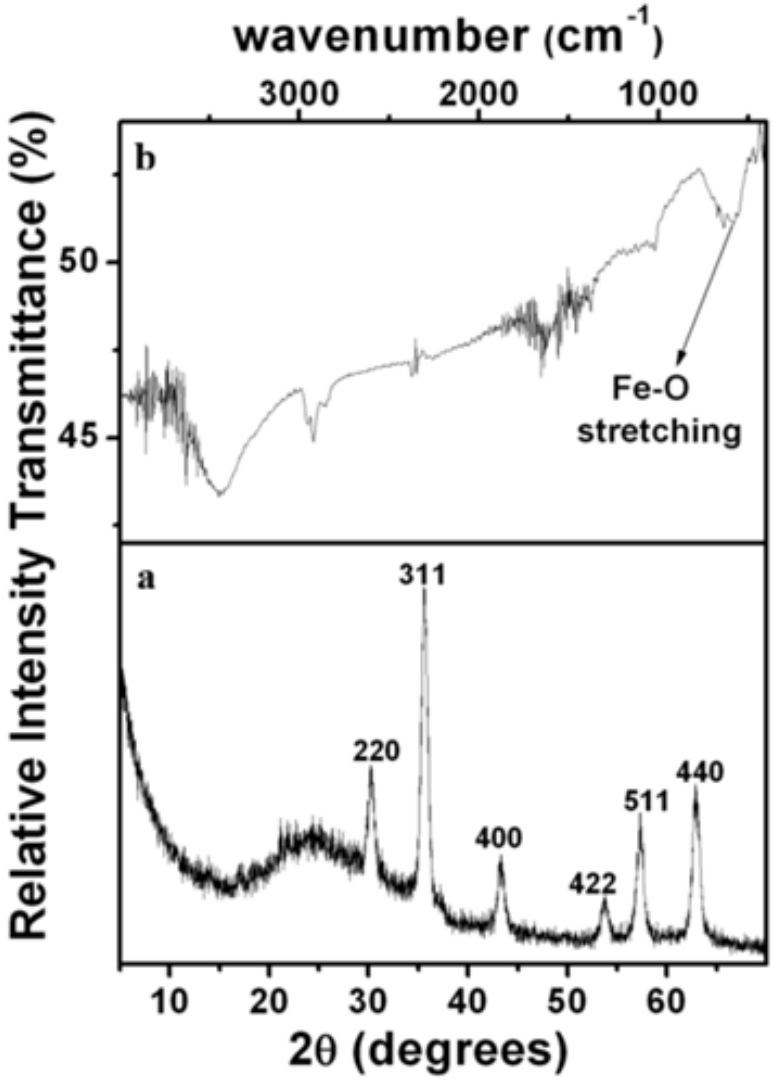

Solvothermal decomposition has emerged as a promising route for obtaining metal oxide nanoparticles [21-23]. This method allows the formation of metal oxides at relatively lower temperatures and products formed will have well defined morphologies. Solvothermal decomposition involves the reaction of precursors in a solvent under high pressure and lower temperatures, allowing for the controlled synthesis of materials with modified properties. Using this principle, colloidal dispersion of the GRDS too was subjected to solvothermal decomposition in both 1-butanol and 1,2-propanediol. While the decomposition was incomplete with the starting LDH present even after 96 h of solvothermal treatment in 1-butanol complete decomposition of the dispersed layers was observed in 1,2-propanediol within 24 h. Figure 3a shows the PXRD pattern of the product obtained on solvothermal decomposition of GRDS in 1,2-propanediol at 200 °C for 24h. All the Bragg reflections of the pattern could be indexed to the cubic γ- Fe_2O_3 (maghemite) phase as reported in JCPDS (39-1346). No other impurity phases including the starting compound, GRDS, are present. From the PXRD line broadening the crystallite size was estimated to be ~11 nm. The IR spectrum of the product (Figure 3b) shows peaks around 650–560 cm^{-1} due to the Fe–O stretching vibrations.

Figure 4: Low (a) and high (b) magnification bright field TEM images, selected area electron diffraction (c) and HRTEM image (d) of γ- Fe_2O_3 nanoparticles obtained on solvothermal decomposition of the GRDS in 1,2-propanediol at 200 ºC.

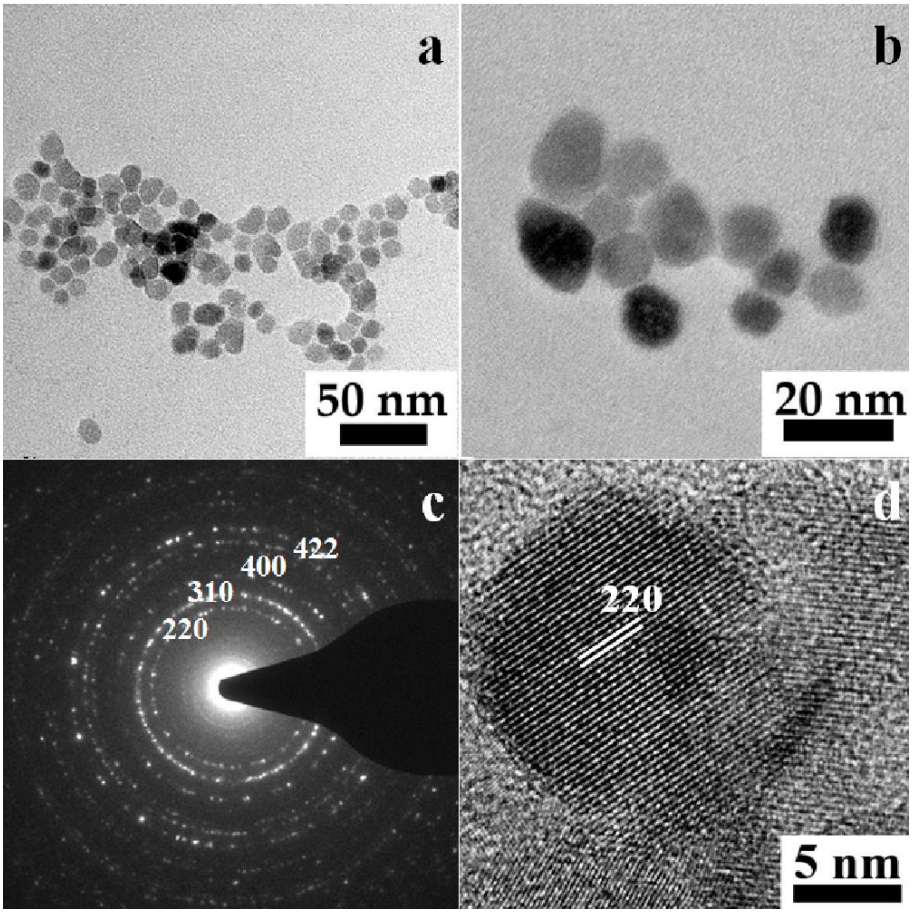

The bright field TEM images of the γ-Fe_2O_3 nanoparticles obtained on solvothermal decomposition of GRDS in 1,2-propanediol at 200 ºC are presented in Figure 4. The low and high magnification images (Figure 4a and b) show the formation of almost monodispersed γ- Fe_2O_3 nanoparticles of ~10 nm diameter. The particle size observed here matches with the crystallite size calculated from the PXRD line broadening suggesting crystalline nature and the narrow size distribution of the γ-Fe_2O_3 nanoparticles. The nanoparticles are roughly spherical in shape. While the diffused rings in selected area diffraction (Figure 4c) suggests the formation of γ-Fe_2O_3 nanoparticles, HRTEM image (Figure 4d) indicates that each γ-Fe_2O_3 nanoparticle is a single crystal.

5. Conclusion

The synthesis of hydroxychloride green rust was carried out using a new hydrolysis procedure. Anion exchange property of green rust has been demonstrated. DS intercalated green rust exfoliates in alcohols and its exfoliation is better than the other LDH analogs in terms of the amount of solid dispersed and the stability of the dispersions. The monolayer colloidal dispersion of the green rust could be converted to monodispersed crystalline γ-Fe_2O_3 nanoparticles by solvothermal decomposition. The bright field TEM images of the γ-Fe_2O_3 obtained confirm that the decomposition of green rust layers resulted in spheroidal nanoparticles.

References

1. G´enin J.-M.R., Refait Ph., Simon L., Drissi S.H., "Preparation and Eh–pH diagrams of Fe (II)–Fe (III) green rust compounds; hyperfine interaction characteristics and stoichiometry of hydroxy-chloride, -sulphate and-carbonate", Hyperfine Interactions, 1998, 111, 313–318.
2. Feitknechtm W., Keller G. Z., "About the Dark Green Hydroxy Compounds of Iron", Journal of Inorganic Chemistry, 1950, 262 (1-5), 61-68.
3. Bernal J. D., Dasgupta, D. R., Mackay A. L., "The Oxides And Hydroxides of Iron and their structural inter-relationships", Clay Minerals Bulletin, 1959, 4, 15.
4. Ponnamperuma F. N., "The Chemistry of Submerged Soils", Advances in Agronomy, 1972, 24, 173.
5. Butler G., Beynon J. G., "The corrosion of mild steel in boiling salt solutions", Corrosion Science, 1967, 7, 385.
6. Abdelmoula M., Philipp R., Drissi S. H., Mihe J. P., Genin J.-M. R., "Mechanisms of formation and structure of green rust one in aqueous corrosion of iron in the presence of chloride ions", Corrosion Science, 1996, 38, 623.
7. Savoye S., Legrand L., Sagon G., Lecomte S., Chausse A., Messina R., Toulhoat P., "Experimental investigations on iron corrosion products formed in bicarbonate/carbonate-containing solutions at 90°C", Corrosion Science, 2001, 43, 2049.
8. Rodriguez J. J. S., Hernandez F. J. S., Gonzalez J. E., "Mathematical and electro-chemical characterisation of the layer of corrosion products on carbon steel in various environments", Corrosion Science, 2002, 44, 2425.
9. Philipp R., Mermet J. B., Bon C., Sabot R., Genin J.-M. R., "Formation of the Fe(II)–Fe(III) hydroxysulphate green rust during marine corrosion of steel", Corrosion Science, 2003, 45, 833.
10. Drissi S. H., Philipp R., Abdelmoula M., Genin J.-M. R., "The preparation and thermodynamic properties of Fe (II)□Fe (III) hydroxide-carbonate (green rust 1); Pourbaix diagram of iron in carbonate-containing aqueous media", Corrosion Science, 1995, 37, 2025.
11. Gehin A., Ruby C., Abdelmoula M., Omar B., Jaafa G., Philipp R., Genin J-M. R., "Coprecipitation of Fe (II) and Fe (III) cations in sulphated aqueous medium and formation of hydroxysulphate green rust", Solid State Sciences, 2002, 4, 61.
12. Trifiro F., Vaccari A., in: Alberti G., Bein T., (Eds.), "Comprehensive Supramolecular Chemistry: Hydrotalcite-Like Anionic Clays (Layered Double Hydroxides)", Elsevier, Oxford, 1996, 7, 251.
13. Ayala-Luis K.B., Koch C. B., Hansen H. C. B., "Intercalation of linear C9–C16 carboxylates in layered FeII–FeIII-hydroxides (green rust) via ion exchange", Applied Clay Science, 2010, 48, 334.
14. Jacobson A. J., in: Alberti G., Bein T. (Eds.), "Comprehensive Supramolecular Chemistry: Colloidal dispersion of compounds with layer and chain structures", Elsevier, Oxford, 1996, 7, 315.
15. Daniel S., Thomas S., "1 - Layered double hydroxides: fundamentals to applications", In Woodhead Publishing Series in Composites Science and Engineering, Layered Double Hydroxide Polymer Nanocomposites, 2020, Pages 1-76
16. Perotti G. F., Bortotti J. R., Lima F. S., Michels L., Dos Santos E. C., Altoe M. A. S., Grassi G., Silva G. J., Droppa R., Fossum J. O., Constantino V. R. L., "Exfoliation of carboxymethylcellulose-intercalated layered double hydroxide in water", Applied Clay Science, 2021, 205, 106005.
17. Liu Z. P., Ma R. Z., Osada M., Iyi N., Ebina Y., Takada K., Sasaki T., "Synthesis, anion exchange, and delamination of Co-Al layered double hydroxide: Assembly of the exfoliated nanosheet/polyanion

composite films and magneto-optical studies", Journal of the American Chemical Society, 2006, 128, 4872– 4880.
18. Takács D., Varga G., Csapó E., Jamnik A., Tomšič M., Szilágyi I., "Delamination of Layered Double Hydroxide in Ionic Liquids under Ambient Conditions" The Journal of Physical Chemistry Letters, 2022, 13, 11850−11856.
19. Hornok V., Erdohelyi A., Dekany I., "Preparation of ultrathin membranes by layer-by-layer (LBL) deposition of oppositely charged inorganic colloids", Colloid and Polymer science, 2006, 284, 611.
20. Ma R., Sasaki T., "Nanosheets of oxides and hydroxides: Ultimate 2D charge-bearing functional crystallites", Advanced Materials, 2010, 22, 5082.
21. Li L., Ma R., Ebina Y., Fukuda K., Takada K., Sasaki T., "Layer-by-Layer Assembly and Spontaneous Flocculation of Oppositely Charged Oxide and Hydroxide Nanosheets into Inorganic Sandwich Layered Materials", Journal of the American Chemical Society, 2007, 129, 8000.
22. Zboril R., Mashlan M., Petridis D., "Iron (III) Oxides from Thermal Processes, Synthesis, Structural and Magnetic Properties, Mössbauer Spectroscopy Characterization, and Applications", Chemistry of Materials, 2002, 14, 969.
23. Lu A-H., Salabas E. L., Schüth F., "Magnetic Nanoparticles: Synthesis, Protection, Functionalization, and Application", Angewandte Chemie International Edition, 2007, 46, 1222 (references therein).
24. Refait P. H., Abdelmoula M., Genin J.–M. R., "Mechanisms of formation and structure of green rust one in aqueous corrosion of iron in the presence of chloride ions", Corrosion Science, 1998, 40, 1547.
25. Misawa T., Suetaka W., Shimodaira S., "Infrared Absorption Spectra and Oxidation of Iron(II) Hydroxide and Green Rust I", Bulletin of the Chemical Society of Japan, 1969, 42, 3339.
26. Snyder R.G., Strauss H.L., Elliger C.A., "Carbon-hydrogen stretching modes and the structure of n-alkyl chains. 1. Long, disordered chains", The Journal of Physical Chemistry, 1982, 86, 5145.
27. MacPhail R. A., Strauss H. L., Snyder R. G., Elliger C. A., "C-H stretching modes and the structure of n-alkyl chains. II: Long, all-trans chains", The Journal of Physical Chemistry, 1984, 88, 334.
28. Adachi-Pagano M., Forano C., Besse J.-P., "Delamination of layered double hydroxides by use of surfactants", Chemical Communications, 2000, 1, 91.
29. Leroux F., Adachi-Pagano M., Intissar M., Chauviere S., Forano C., Besse J.-P., "Delamination and restacking of layered double hydroxides", Journal of Materials Chemistry, 2001, 11, 105.
30. M. Kim, Oh I., Choi H., Jang W., Song J., Kim C. S., Yoo J-W., Cho S., "A solution-based route to compositionally complex metal oxide structures using high-entropy layered double hydroxides", Cell Reports Physical Science, 2022, 3, 100702.
31. Altuntasoglu O., Matsuda Y., Ida S., Matsumoto Y., "Syntheses of Zinc Oxide and Zinc Hydroxide Single Nanosheets", Chemistry of Materials, 2010, 22(10), 3158-3164.
32. Elshof J. E., Yuan H., Rodriguez P. G., "Two-Dimensional Metal Oxide and Metal Hydroxide Nanosheets: Synthesis, Controlled Assembly and Applications in Energy Conversion and Storage", Advanced energy materials, 2016, 6, 1600355.
33. Masashi I., "Solvothermal Synthesis of Metal Oxides", Chapter 11.1.4, Handbook of Advanced Ceramics, Materials, Applications, Processing, and Properties, Second Edition, 2013, Pages 927-948.